Acta Crystallographica Section B
Structural Science
ISSN 0108-7681

Modular crystals as modulated structures: the case of the lillianite homologous series

Luis Elcoro,[a]* J. M. Perez-Mato,[a] Karen Friese,[a] Václav Petříček,[b] Tonči Balić-Žunić[c] and Lars Arnskov Olsen[c]

[a]Dpto de Física de la Materia Condensada, Facultad de Ciencia y Tecnología, Universidad del País Vasco, Apdo 644, Bilbao 48080, Spain, [b]Institute of Physics, Academy of Sciences of the Czech Republic, Na Slovance 2, 182 21 Praha 8, Czech Republic, and [c]Department of Geography and Geology, University of Copenhagen, Øster Voldgade 10, DK-1350 Copenhagen K, Denmark

Correspondence e-mail: luis.elcoro@ehu.es

Received 11 July 2008
Accepted 29 September 2008

The use of the superspace formalism is extended to the description and refinement of the homologous series of modular structures with two symmetry-related modules with different orientations. The lillianite homologous series has been taken as a study case. Starting from a commensurate modulated composite description with two basic subsystems corresponding to the two different modules, it is shown how a more efficient description can be achieved using so-called *zigzag* modulation functions. These linear zigzag modulations, newly implemented in the program *JANA*2006, have very large fixed amplitudes and introduce in the starting model the two orientations of the underlying module sublattices. We show that a composite approach with this type of function, which treats the cations and anions as two separate subsystems forming a misfit compound, is the most appropriate and robust method for the refinements.

1. Introduction

In the last few years structural studies have demonstrated that the superspace formalism, originally developed for the study of incommensurate structures (de Wolff, 1974; Janner & Janssen, 1980*a*,*b*), can also be a very powerful and efficient tool for dealing with the structural properties of commensurate systems with large unit cells (Janssen *et al.*, 1992; van Smaalen, 2007; Janssen *et al.*, 2007). Two recent very extreme examples can be seen in Perez-Mato *et al.* (2006) and Perez-Mato *et al.* (2007). A necessary condition for this type of approach is that the structures have approximate subperiodicities defined by unit cells which are much smaller than the actual unit cell of the structures. Typical examples are series of layered compounds, which, through the stacking of a small number of different types of layers and following composition-dependent sequences, can reach very long periods along the stacking direction (Elcoro *et al.*, 2000). When described using the superspace formalism the approximate subperiodicity created by the layer widths is explicitly and quantitatively used in the structure description. In other words, the approximate atomic positional correlations created by the layered properties of the structure, which are omitted from the conventional crystallographic description, are included in a superspace description, and constitute its basic strength. While in a conventional approach, the difficulty of a quantitative structure analysis increases with the size of the unit cell, due to the increasing number of crystallographically independent atoms, the complexity of the analysis using the superspace method can become essentially independent of the size of the unit cell.

Up to now this approach has been very successful in the study of homologous series of layered compounds (Evain *et*

al., 1998; Perez-Mato *et al.*, 1999; Elcoro *et al.*, 2000, 2001; Boullay *et al.*, 2002; Darriet *et al.*, 2002; Michiue *et al.*, 2005; Michiue *et al.*, 2006; Lind & Lidin, 2003; Orlov *et al.*, 2007). The use of the superspace formalism allows the introduction of a unified description of the whole series, with a number of structural parameters smaller than in a conventional approach and independent of the actual size of the unit cell. It also predicts the three-dimensional space groups which are observed (in general dependent on the specific member of the series), which can be derived directly from the superspace group that describes the symmetry of the whole series.

There are, however, many materials with large unit cells and with underlying approximate subperiodicities which cannot be reduced to layered models. An example would be the so-called modular structures with modules of relatively simple internal structures, which can be combined in various ways and with different orientations (for a recent thorough review see Ferraris *et al.*, 2004). Typical modular structures have modules which are infinite in one or two dimensions and have a form of rods or slabs, respectively. One of the infinite dimensions generally coincides with the short periodicity of the global structure, whereas the periods of the other two crystallographic axes are large and depend on the way the modules combine. Modular structures can present considerable difficulties in structure solution and refinement as they have large unit cells and usually high degrees of pseudosymmetry. Their reciprocal lattices often show strong reflections indicating the sublattices of the modules, flanked by the weaker reflections which are a consequence of the global periodicity. In this respect their diffraction patterns resemble those of commensurately modulated structures.

This resemblance has motivated us to explore the power of the superspace formalism for dealing with modular structures. As modular and modulated structures are in principle two different concepts, a superspace approach to modular structures implies the introduction of a relation between these two different viewpoints. Here we report on the first step in this direction: we have successfully applied the superspace method to the analysis and refinement of modular structures of a series of Pb–Bi–Ag sulfosalts, namely the lillianite homologues. These materials are built from a simple repeat of the same type of modules with two different orientations. In this paper we will show that these structures can indeed be described very efficiently as modulated structures within the superspace formalism, if the usual methodology is extended. It should be mentioned that the superspace framework has also been applied recently to several members of the bismuthine–aikinite modular series (Petříček & Makovicky, 2006), originally described in supercells. However, the character of such modules is quite different: they are rod-like modules instead of the slab-like modules of the lillianite series, which implies a very different superspace description. The rod-like character of the modules permits a standard superspace description as a modulated structure with crenel-like atomic domains and with well defined average positions.

The lillianite homologues are one of the simplest and most investigated series of slab-like modular materials (Makovicky & Karup-Møller, 1977*a*; Ferraris *et al.*, 2004). The general formula for this series is $A_{n+1}X_{n+2}$ with A = Bi, Pb, Ag, Tl, Sb, Nd, Yb, Fe, U, Cu, Eu, Mn, Er, Cr, Ho, Y and X = S, Se (Makovicky & Balić-Žunić, 1993). The most prominent members of this series are the Pb–Bi–Ag sulfosalts. The crystal structures are composed of alternating blocks, the so-called modules. The structure of these modules approximately corresponds to the archetype galena structure (NaCl type). These blocks are parallel to $(3, 1, 1)_{\rm PbS}$ and are in contact through this plane, which is also the mirror plane of the unit-cell twinning operation between two consecutive modules. The structures in this family form homologous series. The homologues vary in the width of the PbS modules which are expressed as the number N of PbS_6 octahedra running diagonally across an individual slab parallel to $[0, 1, 1]_{\rm PbS}$. Each lillianite homologue is denoted as ${}^{N_1,N_2}L$, where N_1 and N_2 are N values for two adjacent modules (Makovicky & Karup-Møller, 1977*a*). We will focus on compounds with the same size for all modules (${}^{N,N}L$ members).

The general chemical formula of the ${}^{N,N}L$ homologue in the series can be expressed as $Pb_{N-1-2x}Bi_{2+x}Ag_xS_{N+2}$. Fig. 1 shows the structure of lillianite, $Pb_3Bi_2S_6$, which is the homologue ${}^{4,4}L$ of the series (Takagi & Takéuchi, 1972). The two galena-like modules within the unit cell can be clearly seen. Other basic members of the series with equal size for the modules are heyrovskyite ($Pb_6Bi_2S_9$) corresponding to the case ${}^{7,7}L$ (Fig. 2), and ourayite ($Pb_4Ag_3Bi_5S_{13}$) which is the case ${}^{11,11}L$ (Makovicky & Karup-Møller, 1977*b*). In general, the cations may have some kind of ordering within the galena modules. We will disregard this possible order for the moment, and

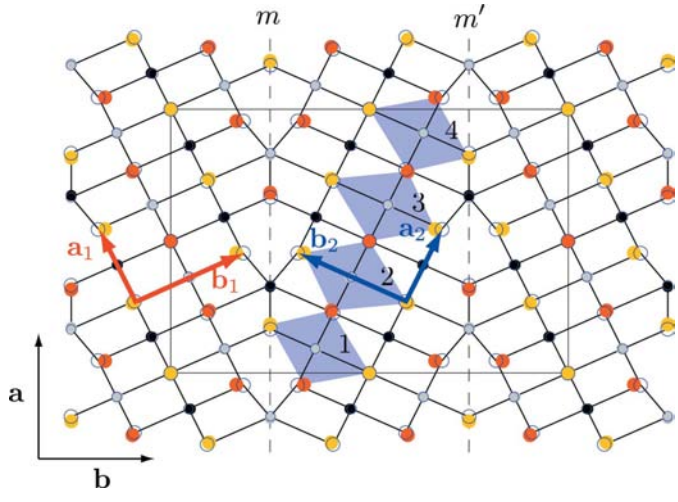

Figure 1
Lillianite projected on the (x, y) plane. Space group *Bbmm*. Larger circles represent the S atoms. Atoms with $z = \frac{1}{2}$ are represented with darker colours than those at $z = 0$. The number of octahedra in the chain of octahedra and the reflection planes relating the two modules are indicated. The unit-cell vectors of the sublattices of the modules in the modular composite approach, given in §4, are indicated. The open circles represent the idealized positions according to these sublattices. Only the x coordinate of the pair of symmetry-independent Pb and S atoms on the contact plane between the modules are free and have been adjusted.

consider that cations are indistinguishable and henceforth will all be termed generically as Pb atoms.

From Figs. 1 and 2 it may seem obvious that the most direct approach to develop a superspace description for these structures would be to consider them as commensurate modulated composite structures, with the two sets of modules with different orientations being the two composite subsystems. In fact, the reciprocal superlattices corresponding to the two orientations of the galena blocks are clearly distinguishable in their diffraction diagrams, as expected in the usual composites (see Fig. 4 in Makovicky & Karup-Møller, 1977*a*). However, these systems have two peculiarities: the two subsystems are symmetry related and some of the atoms are shared by the two subsystems. While the first property, although not present in the usual commensurate and incommensurate composites is not unique, and a few cases are known (Janner & Janssen, 1980*b*; van Smaalen, 1991; Perez-Mato *et al.*, 2006, 2007), the second feature is outside the usual formalism for modulated composites, and represents a formal problem for the application of the methods/programs developed for modulated composite systems.

We will briefly discuss the relationship between modular and modulated structures. This will be followed by some considerations about the choice of the reference sublattices in the lillianite homologous series.

We will then show that it is possible to overcome the problems of the composite approach by introducing an additional subsystem which contains the atoms at the interfaces of the modules. Using this extension, it was possible to refine the structures of lillianite and heyrovskyite satisfactorily using a composite model in four-dimensional space. However, the results of these refinements suggested a different, probably simpler, approach, in which the structures are treated as commensurately modulated structures with linear *zigzag* modulation functions having very large amplitudes. To deal with this type of modulation required the modification of the refinement program *JANA*2006 (Petříček *et al.*, 2006) in order to allow for these zigzag functions as alternative basic modulations. Using these newly introduced functions, the refinement of lillianite and heyrovskyite as modulated structures was straightforward.

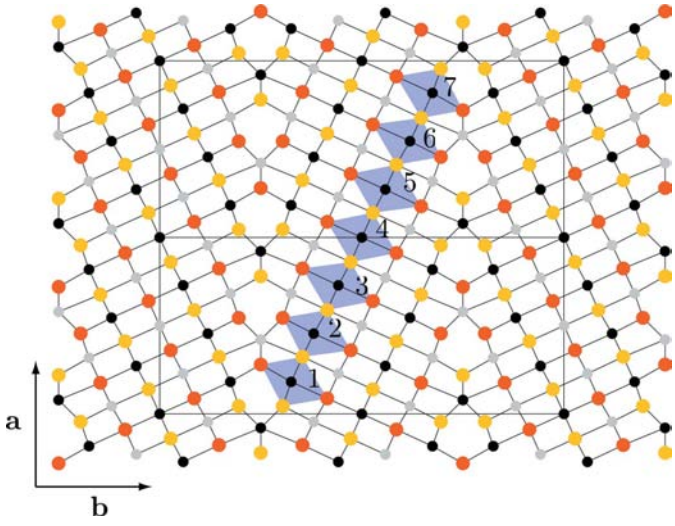

Figure 2
Heyrovskyite projected on the (x, y) plane. Space group *Bbmm*. Larger circles represent the S atoms. Atoms with $z = \frac{1}{2}$ are represented with darker colours than those at $z = 0$. The number of octahedra in the octahedral chains is indicated.

Table 1
Experimental and crystal data for lillianite and heyrovskyite in the conventional three-dimensional setting.

	Lillianite	Heyrovskyite
a (Å)	13.540 (3)	13.701 (2)
b (Å)	20.637 (4)	31.399 (5)
c (Å)	4.1103 (7)	4.1383 (6)
ρ (g cm^{-3})	7.125	7.274
μ (mm^{-1})	75.40	77.24
Crystal colour	Black	Black
Absorption correction	Empirical	Empirical
T_{min}	0.136	0.037
T_{max}	0.316	0.187
No. of measured reflections	6296	5475
No. of unique reflections	1005	756
No. of observed reflections ($I>3\sigma$)	619	455
R_{int}	0.0640	0.0874
$2\theta_{max}$ (°)	61.01	46.50
Range of h, k, l	$-19 \le h \le 19$	$-14 \le h \le 14$
	$-27 \le k \le 29$	$-30 \le k \le 34$
	$-5 \le l \le 5$	$-4 \le l \le 4$

2. Experimental

Two 200 mg powders with the stoichiometric composition of heyrovskyite and lillianite, respectively, were prepared from pure (99.999%) elements of Pb, Bi and S. The powders were filled into quartz tubes which were then evacuated and sealed. The tubes were heated in a tube oven at 573 K. After 24 h the temperature was increased to 873 K and the samples were left for 2 weeks in the oven and finally quenched to room temperature in water. A tabular crystal ($150 \times 65 \times 50$ µm^3) of lillianite and a plate-like crystal ($98 \times 48 \times 15$ µm^3) of heyrovskyite were selected from the resulting samples. X-ray diffraction intensities were collected at 298 K using graphite-monochromated Mo $K\alpha$ radiation on a CCD-equipped Bruker AXS four-circle diffractometer. The orientation and preliminary dimensions of the unit cell were obtained, as prerequisites for intensity integration, using the program *SMART*. Intensity integration was carried out using the *SAINT*+ software and an absorption correction was made with the *SADABS* program. All programs are products of Bruker AXS (Bruker AXS Inc., 2000). More details are shown in Table 1.[1]

[1] Supplementary data for this paper are available from the IUCr electronic archives (Reference: SN5074). Services for accessing these data are described at the back of the journal.

3. Preliminary considerations: modular *versus* modulated structures

When a structure is described as a modular structure the basic point that is being stressed is the presence of certain fragments (modules) that have simple approximate structures with smaller unit cells. These modules are then joined to form the more complex whole structure. When describing homologous series of these structures, the modules can be idealized and used as a reference for the description or determination of the real structures. This approach is not far from the concept of modulated structures, where we also take advantage of the underlying smaller approximate periodicities. However, there is an important additional ingredient that has to be introduced if one wants to describe a modular structure as a modulated one: the idealized lattices that one associates with the modules and which are used as a reference have to be sublattices of the actual lattice of the structure. In other words, in the idealized structure with respect to which the modulation will be defined, disjoint equivalent modules should be translationally coherent according to the sublattice that is defined for the modules and used for the description as a modulated structure.

This point can be illustrated with a simple theoretical example. Let us consider the hypothetical perfect modular crystal represented in Fig. 3. The modules are formed by a perfect rectangular lattice defined by the parameters $\mathbf{A}_o$ and $\mathbf{B}_o$. The periodicity *inter-modules*, which is the only periodicity of the global structure, is shown by **a** and **b**. These **a** and **b** vectors do not correspond to a superlattice of the rectangular lattice of the modules spanned by $\mathbf{A}_o$ and $\mathbf{B}_o$. If we want to describe this structure as a commensurately modulated structure we have to consider an underlying lattice of the modules which is not the idealized orthogonal lattice, but an appropriate oblique sublattice which is *commensurate* with the actual unit cell of the structure, as shown in Fig. 4. The relationship between its unit-cell vectors, $\mathbf{a}_{av}$ and $\mathbf{b}_{av}$, with the actual lattice **a** and **b**, is given by $\mathbf{a} = 3\mathbf{a}_{av} + \mathbf{b}_{av}$ and $\mathbf{b} = -\mathbf{a}_{av} + 5\mathbf{b}_{av}$.

The corresponding diffraction diagram depicted in Fig. 5 shows the set of *main* reflections defined by the lattice spanned by $\mathbf{a}^*_{av}$ and $\mathbf{b}^*_{av}$, and how the remaining reflections, in general much weaker, can be considered satellites generated by a modulation wavevector $\mathbf{q} = \mathbf{b}^* = -\mathbf{a}^*_{av}/16 + 3\mathbf{b}^*_{av}/16$.

The structure with perfect orthogonal modules of Fig. 3 can be obtained from the basic oblique lattice generated by $\mathbf{a}_{av}$ and $\mathbf{b}_{av}$ by introducing a simple linear sawtooth modulation of the atomic positions, as shown in Fig. 6. When represented in superspace, the width Δ of the sawtooth function can be chosen as 11/16; to achieve that 11 of the 16 basic atomic positions within a supercell are occupied. The amplitudes $u_{0,1}$ and $u_{0,2}$ of the sawtooth function are given by $-5.5u_x$ and $5.5u_y$, where $\mathbf{u} = (u_x, u_y)$ is the vector relating the vector $\mathbf{a}_{av}$ of the oblique subcell with the corresponding one, $\mathbf{A}_o$, in the orthogonal subcell of the perfect module: $\mathbf{A}_o = \mathbf{a}_{av} + \mathbf{u}$. The equivalent vector relating $\mathbf{B}_o$ and $\mathbf{b}_{av}$ is given by $-3\mathbf{u}$. This correlation is automatically fulfilled by the superspace description and is forced by the value of the modulation wavevector.

In a real structure the above construction may be seen to be artificial if the oblique sublattice cell strongly deviates from the cell of the ideal archetype structure of the module. However, as shown in Fig. 5, the reciprocal space neatly indicates the adequacy of a description in terms of an oblique subcell rather than the archetypal one. Furthermore, one has to consider that the oblique sublattice is only a virtual reference and, as shown above, the ideal module with the orthogonal subcell can be simply obtained by a linear modulation, which can be introduced *a priori* in the modulated model. In

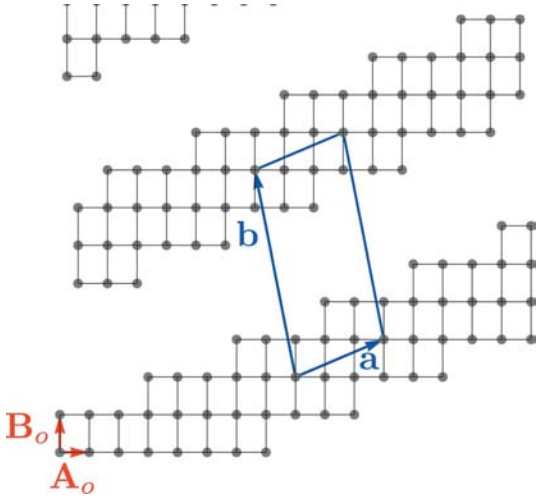

Figure 3
Hypothetical example of a modular structure with identical orthorhombic modules ordered according to an oblique lattice which is not a superlattice of the ideal orthorhombic lattice of the modules.

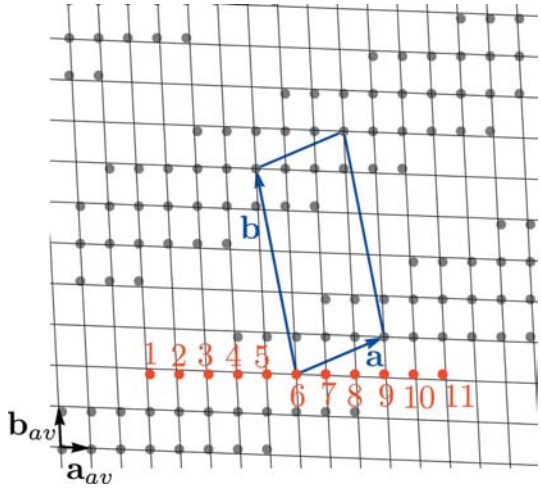

Figure 4
Description of the perfect modular configuration of Fig. 3 as a modulated structure with respect to a basic reference oblique structure. The basic reference lattice is depicted in black. Its unit-cell vectors are given by $\mathbf{a}_{av} = (5/16, -1/16, 0)$ and $\mathbf{b}_{av} = (1/16, 3/16, 0)$ with respect to the actual lattice unit cell indicated in blue. Numeric atomic labels refer to their superspace embedding shown in Fig. 6. This figure is in colour in the electronic version of this paper.

this way, the ideal archetype structure of the modules could be used as reference for the real (modulated) structure of the modules even when it strongly deviates from the oblique sublattice introduced for a modulated description. In any case, the ideal archetype structure of the modules is, in general, an approximate description and is not forced by symmetry in a real structure.

In the lillianite series studied below, the members which are observed experimentally correspond to configurations in which the ideal (orthogonal) subcells of the modules do not deviate much from the oblique ones that make subsequent modules coherent. In other words, the interconnection of the modules within the structures is such that the ideal archetype sublattices of the modules only require a small deformation to become commensurate with the periodicity of the actual global structure.

In general, the superspace formalism can have an important flexibility in the choice of setting, each of which would change the meaning of the internal subspace (Elcoro & Perez-Mato, 1996). Furthermore, the description of commensurate structures even has a much larger flexibility. One can describe the same structure using different choices for the superspace symmetry, the basic structure, the modulation wavevector *etc.* In the following, we will consider several possibilities. In the end, the decision about the most appropriate description will emerge from the comparison of the resulting modulation functions corresponding to the individual models. The best model will be the one that describes the modulations with the simplest functions and where the least variation is observed between different members of the homologous series.

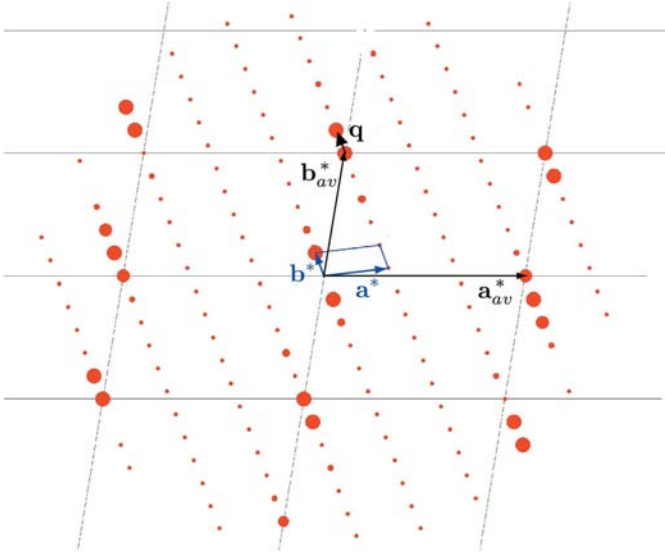

Figure 5
Scheme of the diffraction diagram of the hypothetical structure shown in Fig. 3. The lattice of main reflections defined by the vectors $\mathbf{a}^*_{av}$ and $\mathbf{b}^*_{av}$ is indicated together with the choice of the modulation vector $\mathbf{q} = \mathbf{b}^*$, for a description as a modulated structure. Note that the diagram does not have any qualitative signature revealing the orthogonal lattices of the modules of the structure in direct space.

4. Preliminary considerations: approximate reference sublattices in $^{N,N}L$ members of the lillianite series

The approximate sublattices of the two modules in lillianite can be described by two body-centred subcells with vectors $\mathbf{a}_1 = (3/11, -1/11, 0)$, $\mathbf{b}_1 = (2/11, 3/11, 0)$, $\mathbf{c}_1 = (0, 0, 1)$ for one block and $\mathbf{a}_2 = (3/11, 1/11, 0)$, $\mathbf{b}_2 = (2/11, -3/11, 0)$ and $\mathbf{c}_2 = \mathbf{c}_1 = (0, 0, 1)$ for the second modulus, both sublattices being symmetry-related by a mirror plane m_y (here and in the following we are using the setting of the experimental *Bbmm* structure; Takagi & Takéuchi, 1972; Takeuchi & Takagi, 1974; and its unit-cell vectors as a reference). Fig. 1 shows the idealized structure of lillianite using these sublattices (open circles in the figure). Only the atoms on the connecting plane between two consecutive modules are displaced from the idealized positions given by the subcells defined above. For heyrovskyite the analogous subcell vectors are $\mathbf{a}_1 = (5/18, -1/18, 0)$, $\mathbf{b}_1 = (3/18, 3/18, 0)$, $\mathbf{c}_1 = (0, 0, 1)$, and those related by a mirror m_y.

In general, the two subcells fulfill the relation

$$3\mathbf{a}_i + \mathbf{b}_i = (1, 0, 0) \qquad (1)$$

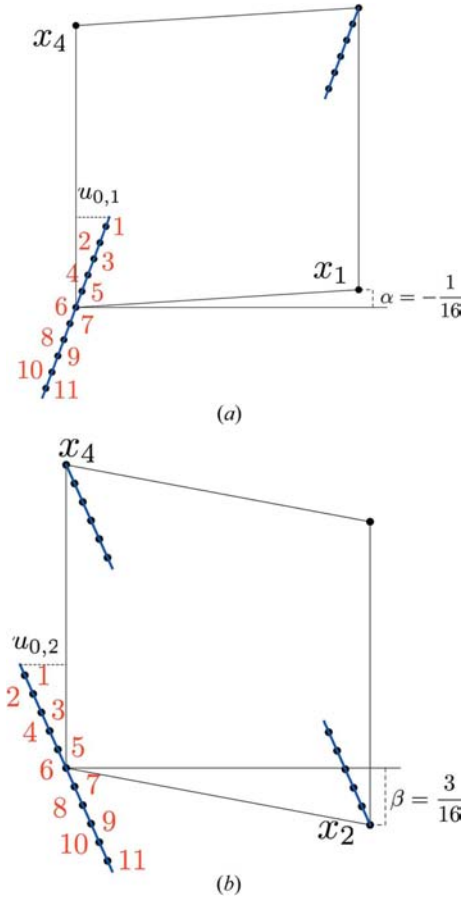

Figure 6
Sawtooth function along (*a*) x_1 and (*b*) x_2 describing the orthogonal perfect modules of Fig. 3, using the oblique basic lattice and the modulation wavevector indicated in Figs. 4 and 5. Points correspond to the actual atomic positions realised in the structure. Numeric labels correspond to those indicated in Fig. 4.

Table 2
Best (n, p) values for ${}^{N,N}L$ members of the broad lillianite family.

(n', p') values are the solution of equations (4) and (5). (n, p) are rounded-up values of (n', p') [for $N = 2$ two different choices of (n, p) were used for comparison]. $a_1, b_1, c_1, \alpha, \beta, \gamma$ are the parameters of the unit cell of the sublattice defined by equations (2), calculated from the experimental unit cell of the compound indicated in the last column. The a_1/c_1 and b_1/c_1 values for an ideal undistorted sublattice are 1 and $2^{1/2} \simeq 1.414$, respectively.

N	n', p'	n, p	a_1/c_1	b_1/c_1	γ	β	α	Compound
1	1.09, 1.64	1,2	1.003	1.215	90.6	90	90	$CuEu_2S_3$ [a]
2	1.45, 2.18	1,2	1.063	1.517	81.4	90	90	$MnEr_2S_4$ [b]
2	1.45, 2.18	2,2	0.931	1.512	96.5	90	90	$MnEr_2S_4$ [b]
3	1.81, 2.73	2,2	0.860	1.499	90.6	94.9	92.8	$TlSb_3S_5$ [c]
4	2.18, 3.27	2,3	1.007	1.488	87.1	90	90	$Pb_3Bi_2S_6$ [d]
5	2.55, 3.81	–	–	–	–	–	–	–
6	2.91, 4.36	–	–	–	–	–	–	–
7	3.27, 4.91	3,5	1.012	1.379	91.1	90	90	$Pb_6Bi_2S_9$ [d]
8	3.64, 5.45	–	–	–	–	–	–	–
9	4, 6	–	–	–	–	–	–	–
10	4.36, 6.55	–	–	–	–	–	–	–
11	4.72, 7.09	5,7	0.990	1.412	88.1	90	90	$Pb_4Ag_3Bi_5S_{13}$ [e]
12	5.09, 7.64	–	–	–	–	–	–	–
13	5.45, 8.18	–	–	–	–	–	–	–
14	5.82, 8.72	–	–	–	–	–	–	–
15	6.18, 9.27	–	–	–	–	–	–	–

References: (*a*) Lemoine *et al.* (1986); (*b*) Landa-Canovas & Otero-Diaz (1992); (*c*) Gostojić *et al.* (1982); (*d*) this work; (*e*) Makovicky & Karup-Møller (1984).

so that the size of the unit cell of the whole system along the x direction is common for the whole homologous series. For a generic member of the series, the approximate B-centred subcells of the two modules can be generated by the vectors

$$\begin{aligned}\mathbf{a}_{1,2} &= \left(\frac{p}{3p+n}, \mp\frac{1}{3p+n}, 0\right)\\ \mathbf{b}_{1,2} &= \left(\frac{n}{3p+n}, \pm\frac{3}{3p+n}, 0\right)\\ \mathbf{c}_{1,2} &= (0, 0, 1).\end{aligned} \tag{2}$$

The integers n and p in the equations above define the second necessary commensurability relation of the subperiodicity of the modules with the actual lattice of the global structure, given by

$$p\mathbf{b}_i - n\mathbf{a}_i = (0, \pm 1, 0). \tag{3}$$

Lillianite, which is the ${}^{4,4}L$ homologue of the series, corresponds to $(n, p) = (2, 3)$, while for heyrovskyite and ourayite, $(n, p) = (3, 5)$ and (5,7), respectively. To obtain these generic idealized sublattices we have assumed the commensurability of the sublattices with the lattice of the global subsystem, as explained in the previous section. This condition together with (1) is sufficient for restricting the possible idealized sublattices of the modules to the form given by (2). It is important to note that the reference sublattices that we associate with the modules using (2) are in general not strictly orthogonal. In contrast to the usual modular description of the series (Makovicky & Karup-Møller, 1977*a*), in a modulated description the sublattices of modules with the same orientation are forced to match exactly with each other and with the actual lattice of the global system, at the cost of these reference galena sublattices being strained.

This strain can be readily calculated comparing the ideal PbS archetype unit cell with that generated by the defined vectors $\{\mathbf{a}_1, \mathbf{b}_1, \mathbf{c}_1\}$. As can be seen in Fig. 1, this strain is very small.

In general, and for any member ${}^{N,N}L$ of the series, one can systematically derive which choice of the (n, p) parameters yields the least strained module sublattices, as defined by (2). This is discussed in detail in *Appendix A*. There it is shown that, for a given N and considering an orthogonal unit cell for the global structure, (2) would only yield sublattices unstrained with respect to the PbS archetype if the integers n and p defining the sublattice fulfill

$$n/p = 2/3. \tag{4}$$

In addition, under these ideal conditions, these two integers would be related to N by the relation

$$3p + n = 2N + 4. \tag{5}$$

These two equations have in general non-integer solutions for (n, p) except for very specific N values ($N = 9, 20, \ldots$). The integers $(2, 3)$ chosen above for lillianite satisfy (4), while deviate from (5) by one unit. On the other hand, in the case of heyrovskyite the pair $(n, p) = (3, 5)$ satisfies (5), but its ratio has a minimal deviation from the ideal value given by (4). These deviations lead to small strains in the reference sublattices defined in (2). In general, for a given N, the best choice for (n, p) can be derived from the non-integers solutions, (n', p'), of the corresponding equations (4) and (5), taking the integer values (n, p) that are closer to these (n', p') values. Table 2 lists the results for the lowest N values. It can be seen that the known sulfosalts ${}^{N,N}L$ of the lillianite series correspond to N values for which the non-integer values (n', p') are rather close to integer values. This seems to indicate that the stable phases are those allowing for the least distorted archetype sublattices. Nevertheless, it is remarkable that the member of ${}^{9,9}L$, where a sublattice given by $(n, p) = (4, 6)$ could fulfill exactly the two matching conditions and therefore

could accommodate a perfect galena structure as a sublattice, has never been reported.

As can be seen in Table 2, the lower homologues of the broader structural family, which however do not belong to Pb/Bi sulfosalts, cope with somewhat higher distortions; *e.g.* for $^{2,2}L$ homologues the choice of (n, p) values becomes ambiguous, with two possible choices requiring relatively large distortions of the sublattice. The value of $3p + n$ due to the integer truncation can vary between $2N + 2$ up to $2N + 5$. The values for the observed homologues *sensu strictu* of lillianite being $2N + 3$ (for lillianite) and $2N + 4$ (for heyrovskyite and ourayite).

5. Description of $^{N,N}L$ members of the lillianite homologous series as commensurate modular composites

The reciprocal lattices associated with the sublattices of the modules discussed in the previous section, and which we will use in a composite description of the lillianite series, are determined by the chosen pair of integers (n, p). The corresponding reciprocal unit cells are given by

$$\begin{aligned}\mathbf{a}^*_{1,2} &= (3, \mp n, 0)\\ \mathbf{b}^*_{1,2} &= (1, \pm p, 0)\\ \mathbf{c}^*_{1,2} &= (0, 0, 1),\end{aligned} \tag{6}$$

where we use the reciprocal unit cell of the observed global structure as a reference. Equations (6) define two reciprocal lattices describing the main reflections of the two modules in a composite description. Following the usual approach for composite structures in superspace (Janssen *et al.*, 1992; van Smaalen, 1991, 2007), the Bragg reflections can be indexed with four indices in the form

$$\mathbf{H} = h_1\mathbf{a}^*_1 + k_1\mathbf{b}^*_1 + l_1\mathbf{c}^*_1 + m_1\mathbf{q}_1 = h_2\mathbf{a}^*_2 + k_2\mathbf{b}^*_2 + l_2\mathbf{c}^*_2 + m_2\mathbf{q}_2, \tag{7}$$

where the modulation wavevectors $\mathbf{q}_1$ and $\mathbf{q}_2$ are usually the basis vector of the reciprocal lattice of subsystems 2 and 1, respectively. As $3\mathbf{b}^*_1 - \mathbf{a}^*_1 = -(3\mathbf{b}^*_2 - \mathbf{a}^*_2) = (0, 3p + n, 0)$, a natural choice for $\mathbf{q}_1$ and $\mathbf{q}_2$ may seem $\mathbf{b}^*_2$ and $\mathbf{b}^*_1$, respectively, or equivalent ones. However, as the two subsystems are commensurate there are in fact other possibilities for the choice of modulation wavevector which are more appropriate.

As an example, Fig. 7 shows a scheme of the $(h, k, 0)$ plane of the diffraction diagram of heyrovskyite, where the lattices of main reflections corresponding to the two subsystems are highlighted. Although the extinction condition corresponding to the *B* centring hides these underlying superlattices, they can nevertheless be distinguished as corresponding to rather strong reflections. Although the usual intensity hierarchy between main reflections and pure satellites does not exist here, one can see the more intense reflections clustered around both sets of main reflections. It is clear from the figure that the natural choice of the modulation wavevectors should be along the $\mathbf{b}^*_{av}$ direction. $\mathbf{b}^*_1 - \mathbf{b}^*_2 = (0, 2p, 0)$, *i.e.* $10\mathbf{b}^*$ in the case of heyrovskyite, fulfills this condition, and will be in accordance with the usual choice in composites. However, as suggested by Fig. 7, this modulation wavector is not the optimum choice and in fact, if used, does not yield simple atomic domains in superspace. This is not surprising as we are dealing with a structure that does not fulfill one of the basic assumptions in standard composites, namely that the modulation of the composite subsystems originates from their mutual interaction. In the present case, the basic modulation describes the periodic sequence of the two modules. This sequence is not produced by mutual interactions of the modules, but rather has its origin in the cation deficiency of the system with respect to the galena composition. The deficiency is accommodated in the interfaces between consecutive modules and, hence, the basic modulation has a different origin than in a conventional composite. As suggested by the scheme in Fig. 7, the best choice for the modulation wavevector is $\mathbf{q}_1 = -\mathbf{q}_2 = \mathbf{b}^* = (0, 1, 0)$. This wavevector is consistent with the supercell of modules 1 and 2, realised in the real structure, and what is most important, the atomic positions when embedded in superspace aggregate into large atomic domains.

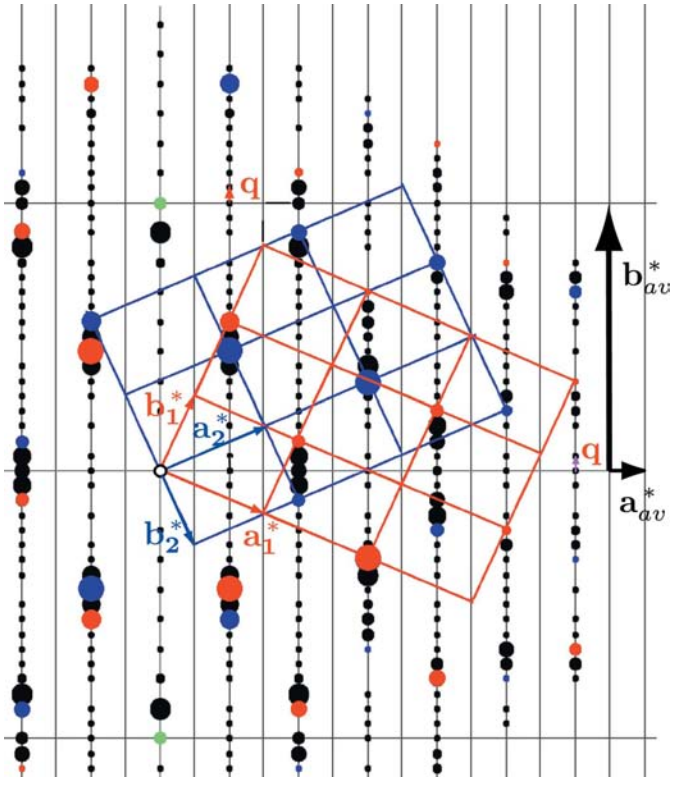

Figure 7
Scheme of the diffraction pattern of heyrovskyite on the plane $(h, k, 0)$. The lattices of main reflections corresponding to the two subsystems of the modular composite approach defined in subsection 5.1 are outlined. Reflections which are common to both sets are indicated in green. The chosen modulation wavector is also indicated.

Table 3
Operations defining the superspace groups employed in the superspace description of a lillianite $^{N,N}L$ member, when choosing the basic cell such that $\beta = 1/(2N+4)$ (first column) or $\beta = 1/(2N+3)$ (second column).

$Bmmm(0,\beta,0)s00$	$Bbmm(0,\beta,0)s00$
(x_1,x_2,x_3,x_4), $(\frac{1}{2}+x_1,x_2,\frac{1}{2}+x_3,x_4)$ + (x_1,x_2,x_3,x_4)	(x_1,x_2,x_3,x_4), $(\frac{1}{2}+x_1,x_2,\frac{1}{2}+x_3,x_4)$ + (x_1,x_2,x_3,x_4)
$(-x_1,-x_2,x_3,-x_4)$	$(-x_1,-x_2,x_3,-x_4)$
$(-x_1,x_2,-x_3,\frac{1}{2}+x_4)$	$(-x_1,\frac{1}{2}+x_2,-x_3,\frac{1}{2}+x_4)$
$(x_1,-x_2,-x_3,\frac{1}{2}-x_4)$	$(x_1,\frac{1}{2}-x_2,-x_3,\frac{1}{2}-x_4)$
$(-x_1,-x_2,-x_3,-x_4)$	$(-x_1,-x_2,-x_3,-x_4)$
$(x_1,x_2,-x_3,x_4)$	$(x_1,x_2,-x_3,x_4)$
$(x_1,-x_2,x_3,\frac{1}{2}-x_4)$	$(x_1,\frac{1}{2}-x_2,x_3,\frac{1}{2}-x_4)$
$(-x_1,x_2,x_3,\frac{1}{2}+x_4)$	$(-x_1,\frac{1}{2}+x_2,x_3,\frac{1}{2}+x_4)$

Table 4
Three-dimensional space groups of commensurate structures with superspace group $Bmmm(0,\beta,0)s00$ with $\beta = 1/M$, $M = 2N+4$ or $Bbmm(0,\beta,0)s00$ with $\beta = 1/M$, $M = 2N+3$, for different choices of the real space section, t and $i = 0, 1, \ldots, M-1$.

Section	Space group
$t = i/M$	$Bbmm$
$t = 1/(2M) + i/M$	$Bbmm$
$t =$ general	$Bb2_1m$

The superspace description of a composite requires the introduction of the matrices W_i, which define the indexing basis of reciprocal vectors employed in each subsystem with respect to a common basis of reciprocal vectors (van Smaalen, 1991). In this case it is convenient to use as a common basis an orthorhombic cell in accordance with the supercell of the global structure. This is in contrast to the usual approach of using one of the subsystems as a common basis. Furthermore, the atoms on the interface between modules are shared by the two subsystems, producing a formal problem not encountered up to now in the superspace treatment of composites. Because of this, these atoms can only be consistently introduced in the *JANA* program (Petříček *et al.*, 2006) as an extra subsystem, associated with the common orthogonal cell used as a reference.

Therefore, for a given $^{N,N}L$ member of the series we choose as a basis for this common reference subsystem (henceforth termed subsystem 0) the following vectors (always referred to the reciprocal cell of the experimental structure)

$$\begin{aligned}\mathbf{a}_o^* &= \mathbf{a}^* = (1,0,0)\\ \mathbf{b}_o^* &= M\mathbf{b}^* = (0,M,0)\\ \mathbf{c}_o^* &= \mathbf{c}^* = (0,0,1)\\ \mathbf{q}_o &= \mathbf{b}^* = (0,1,0) = \frac{1}{M}\mathbf{b}_o^*,\end{aligned} \tag{8}$$

with M being either $(2N+3)$ or $(2N+4)$ for the cases investigated here. For a fixed N, both choices of M are possible, and as we will see below they imply the use of different superspace-group symmetries.

5.1. Choice $M = 2N + 4$

Let us consider first the choice $M = 2N+4$. The bases of the subsystems are defined by a pair of integers (n,p) fulfilling either $3p+n = 2N+4$ or $3p+n = 2N+3$, and equations (6). Considering (6) and (8), this implies that the matrix W_1 for subsystem 1, expressing the reciprocal basis (6) in terms of the basis (8) can be given by

$$W_1 = \begin{pmatrix} 3 & -1 & 0 & 3p \\ 1 & 0 & 0 & p \\ 0 & 0 & 1 & 0 \\ 0 & 0 & 0 & 1 \end{pmatrix} \quad \text{if } 3p+n = M \tag{9}$$

or

$$W_1 = \begin{pmatrix} 3 & -1 & 0 & 3p+1 \\ 1 & 0 & 0 & p \\ 0 & 0 & 1 & 0 \\ 0 & 0 & 0 & 1 \end{pmatrix} \quad \text{if } 3p+n = M-1. \tag{10}$$

The inverse of W_1 is also an integer matrix, indicating that any diffraction peak can be indexed in any of the two bases adapted to each subsystem, as expected in a composite. The matrix W_2 of subsystem 2 (the second module) is symmetry related to W_1 and, according to equations (6), can be obtained by changing the signs of the second and fourth columns of W_1. On the other hand, W_0 for subsystem 0 is the identity, as it is described in the reciprocal basis (8). $\mathbf{q}_o$ is taken as the modulation wavevector for the three subsystems.

The superspace group to be used (in the setting of subsystem 0) is $Bmmm(0,\beta,0)s00$, as described in Table 3. As shown in Table 4, this superspace symmetry is fully consistent with the three-dimensional space group of the structure. The atomic domains defining the ideal modular structure are listed in Table 5. As the atomic domains of subsystem 2 are related by a symmetry operation with those of subsystem 1, the list of independent atomic domains includes just atoms of subsystems 0 and 1. For N odd, the three-dimensional structure corresponds to $t = 0$ or equivalent sections (see Table 4), resulting in the location of a Pb atom at the inversion centre, while for N even, a section $t = \frac{1}{2M}$ or equivalent (see Table 4) generates the three-dimensional structure, which then has the inversion centre on a sulfur atom. This different choice of t depending on the parity is in fact symmetry forced, because the other possible high-symmetry t sections would cut the atomic domains at their mathematical border, breaking the assumed symmetry or producing half occupied atomic positions.

Figs. 8 and 9 depict the (x_1,x_4) and (x_2,x_4) projections of the superspace unit cell (in the setting of subsystem 0) of this initial composite model for lillianite $[(n,p) = (2,3)]$ and heyrovskyite $[(n,p) = (3,5)]$, respectively. These figures show the atomic domains in superspace that describe the starting model with the module sublattices given by equation (2).

Table 5
Atomic domains in superspace defining an ideal $^{N,N}L$ member of the lilllianite homologous series within the modular composite model (choice $M = 2N + 4$ and superspace group of the first column of Table 3).

The positions of the centres of the atomic domains plus their widths Δ along x_4 are listed. Parameters of subsystem 2 are directly related with those of subsystem 1 by the superspace group symmetry. The parameter n has been defined in §4, equation (2). Parameters printed in bold are refinable. The matrices of the zeroth, first and second subsystems are the identity, $W_1 = W_+$ and $W_2 = W_-$, respectively.

Atom	Subsystem	x_1^0	x_2^0	x_3^0	x_4^0	Δ	Point symmetry	Displacive modulation
S0	0	$(\mathbf{7n-6})/\mathbf{12}$	1/2	0	1/4	$1/(2N+4)$	1	Not used
Pb0	0	$(\mathbf{7n-10})/\mathbf{12}$	1/2	0	1/4	$1/(2N+4)$	1	Not used
S1	1	0	1/2	0	0	$(N+1)/(2N+4)$	$112/m$	(sin,sin,0)
Pb1	1	0	0	0	0	$N/(2N+4)$	$112/m$	(sin,sin,0)

Lillianite	Heyrovskyite
$W_\pm = \begin{pmatrix} 3 & \mp1 & 0 & \pm10 \\ 1 & 0 & 0 & \pm3 \\ 0 & 0 & 1 & 0 \\ 0 & 0 & 0 & \pm1 \end{pmatrix}$	$W_\pm = \begin{pmatrix} 3 & \mp1 & 0 & \pm15 \\ 1 & 0 & 0 & \pm5 \\ 0 & 0 & 1 & 0 \\ 0 & 0 & 0 & \pm1 \end{pmatrix}$

Using this superspace model one can construct the idealized structure of lillianite with perfect module sublattices that was shown in Fig. 1. Of course, the real structure requires additional displacive modulations to be refined. Note that for lillianite, the fact that $M = 12$ does not coincide with $3p + n$ implies that the atomic domains on the (x_2, x_4) plane are oblique or sawtooth-like when seen in the setting of subsystem 0, while for heyrovskyite where $M = 18 = 3p + n$, they are vertical, as in the W_1 setting. In lillianite the sawtooth domains have the direction [1,1] on the plane (x_2, x_4). This corresponds to the fact that the atoms of the ideal modules we are building with this construction have y coordinates of the type $i/11$ and not $i/12$ (i integer). On the other hand, the atomic domains of heyrovskyite (Fig. 9) are vertical along x_4 on the projection (x_2, x_4). This means that the ideal y coordinates of both Pb and S in the two consecutive modules are given by fractions of the type $i/18$. We will see below, however, that the real structures of both compounds, when refined starting from the models depicted in Figs. 8 and 9 reach in both cases configurations which can be considered intermediate between the two idealized models represented by Figs. 8(a) and 9(a), so differences between the two starting models are blurred.

The composite character of the structure can be seen in the (x_1, x_4) projection (Figs. 8b) and 9b), where the S2 and Pb2 atomic domains belong to the second module (subsystem 2), and are obtained from those of the first module (subsystem 1) by the given superspace symmetry. The domains in consecutive modules form a zigzag pattern when depicted in this orthogonal common setting corresponding to subsystem 0. The resulting x atomic coodinates are those necessary to produce the oblique ideal galena modules. This zigzag pattern is in fact fully isomorphous to the pattern formed by rows of atoms on the plane (x, y) of the real three-dimensional structure.

In Figs. 8 and 9, one can also see that the above superspace description stresses the cation deficiency as the basic feature of the structure. The S domains occupy the whole x_4 interval yielding a total of $M(= 2N + 4)$ atoms on the plane $z = 0$, while the Pb domains yield $2N + 2$ occupied atomic positions. Two pairs of Pb and S atoms with the same y coordinate (the Pb0 and S0 atomic domains for subsystem 0) are distributed uniformly along y and fulfill a closeness condition in superspace, directly related with the modulus of $\mathbf{q}_o$, equal to the x_4 width of these atomic domains.

In the following, we shall term the above superspace description of lillianites a modular composite model. It can be used to construct the ideal structure of any member of the homologous series with *JANA*2006. We only have to introduce the corresponding matrices W_i and the widths of the atomic domains as given in Table 5, and adjust the free x coordinates of the S0 and Pb0 atoms. As an example, Fig. 10 shows the resulting structure for the member $^{13,13}L$ member with (n, p) chosen as (5,8).

5.2. Choice $M = 2N + 3$

The composite description described above has been obtained choosing the basic unit cell of the reference subsystem 0 with $\mathbf{b}_o = M\mathbf{b} = (2N + 4)\mathbf{b}$, which implies that the modulation wavevector, common for the three subsystems, is given by $\mathbf{b}_o^*/(2N + 4)$. As mentioned above, an alternative composite superspace description results when using $M = 2N + 3$ ($\mathbf{q} = \mathbf{b}_o^*/(2N + 3)$). The matrix W_1 is then the same as in the previous case if $3p + n = M$ and

$$W_1 = \begin{pmatrix} 3 & -1 & 0 & 3p-1 \\ 1 & 0 & 0 & p \\ 0 & 0 & 1 & 0 \\ 0 & 0 & 0 & 1 \end{pmatrix} \quad \text{if } 3p + n = M + 1. \quad (11)$$

Table 8 in the supplementary material summarizes this alternative choice. Also the description of the atomic domains in the setting of the subsystem 0 becomes reversed with respect to the previous choice of M. In the case of heyrovskyite, M does not coincide with $3p + n$ and the atomic domains are oblique or sawtooth-like, while for lillianite where $M = 11 = 3p + n$ they are vertical as in the W_1 setting. This

could be taken as an indication that this choice is more natural for N even. However, as mentioned above, the actual refined structures described in detail below have displacive modulations which are large enough to make the description independent of the parity of N.

6. Refinement of lillianite and heyrovskyite within a superspace modular composite model

The refinements of lillianite and heyrovskyite within the modular composite model were started from the idealized composite model described in the previous section and Table 5. It should be noted that in this approach all cations have been assumed to have a Pb scattering factor. This is, in fact, in accordance with the standard refinement of the sulfosalt crystal structures, because of the negligible difference in the scattering factors of Pb and Bi in the conventional X-ray diffraction. Crystal chemical analysis (Pinto *et al.*, 2006) suggests a pure Pb site for the Pb0 domain and a mixed Pb/Bi occupancy for the symmetrically independent sites contributing to the present domain Pb1. Apart from the atomic displacement parameters (ADPs), the only parameters which are refinable in the starting basic non-modulated structure are the x coordinates of atoms Pb0 and S0, belonging to subsystem 0. These parameters and the ADPs in the basic structure were adjusted first. In subsequent refinement cycles the atomic modulation functions were introduced. For the lillianite compound, the maximum number of harmonics (two) consistent with the commensurate character of the structure was used for atoms S1 and Pb1. In the case of heyrovskyite, the maximum number of harmonics is three and four for Pb1 and S1, respectively. However, in the final refined model, three harmonics were included for both atoms, as the inclusion of the fourth harmonic for the S1 atom did not improve the results significantly. For the sake of comparison, the structure was also refined in three-dimensional space (space group *Bbmm*). The transformation of the four-dimensional model to

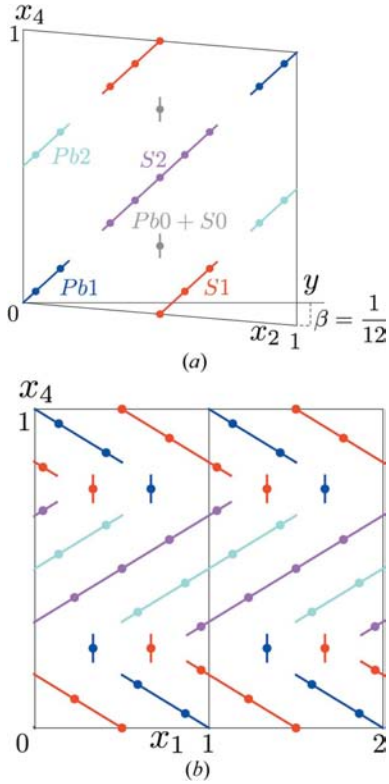

Figure 8
Projection (*a*) (x_2, x_4) and (*b*) (x_1, x_4) of the atomic domains with $x_3 = 0$ for the modular composite model of lillianite with ideal modules. The setting used for the superspace and the structural parameters are given in Table 5 for $N = 4$ and $n = 2$. Red and magenta represent S domains in subsystems 1 and 2, respectively, while blue and cyan represent Pb domains in subsystems 1 and 2, respectively. The grey domains in (*a*) correspond to the superposition of S0 and Pb0 domains.

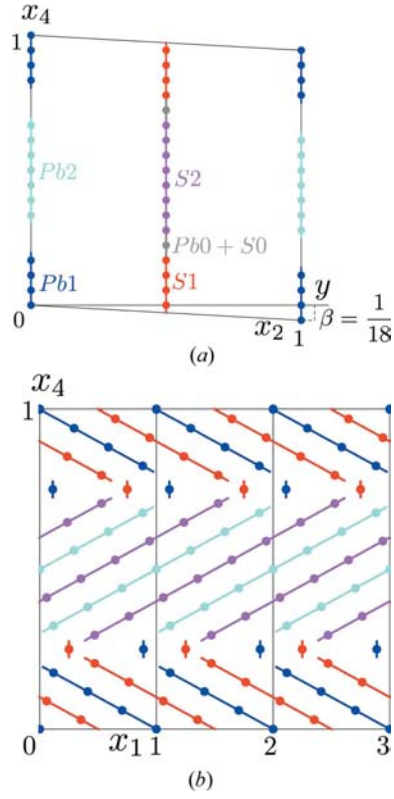

Figure 9
Projection (*a*) (x_2, x_4) and (*b*) (x_1, x_4) of the atomic domains with $x_3 = 0$ for the modular composite model of heyrovskyite with ideal modules. The setting used for the superspace and the structural parameters are given in Table 5 for $N = 7$ and $n = 3$. Colour labels are those of Fig. 8.

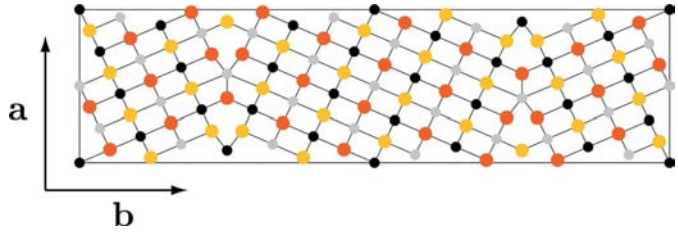

Figure 10
Ideal structure of the $^{13,13}L$ member of the lillianite homologous series constructed with the modular composite model described in §5.1.

Table 6
Results of the three-dimensional structure refinements and superspace refinements in the modular composite and misfit composite descriptions, for the lillianite and heyrovskyite structures.

R factors are given for all reflections and, for four-dimensional refinements, also for main ($m = 0$) and satellite reflections up to $m = 4$ order.

	Lillianite composite	Lillianite misfit	Lillianite three-dimensional	Heyrovskyite composite	Heyrovskyite misfit	Heyrovskyite three-dimensional
Independent/observed ($I>3\sigma$) reflections	1004/619	1004/619	1004/619	756/455	756/455	756/455
Parameters	26	26	38	30	36	56
R(obs)/R(all)						
All	0.0496/0.0752	0.0484/0.0726	0.0462/0.0699	0.0421/0.0795	0.0405/0.0779	0.0387/0.0757
$m = 0$	0.0508/0.0816	0.0514/0.0855		0.0478/0.0679	0.0552/0.0973	
$m = 1$	0.0527/0.0724	0.0460/0.0657		0.0426/0.0763	0.0367/0.0876	
$m = 2$	0.0505/0.0810	0.0426/0.0696		0.0343/0.0611	0.0321/0.0706	
$m = 3$	0.0475/0.0691	0.0461/0.0621		0.0431/0.0885	0.0397/0.0664	
$m = 4$	0.0477/0.0704	0.0589/0.0822		0.0450/0.0920	0.0387/0.0805	
GoF(obs)/GoF(all)	2.12/1.71	2.10/1.70	2.05/1.65	1.59/1.41	1.65/1.45	1.48/1.32

the corresponding three-dimensional model (easily achieved due to the commensurability of the composite model) shows that – taking into account the standard deviations – all refined parameters are comparable in the three- and four-dimensional refinements.

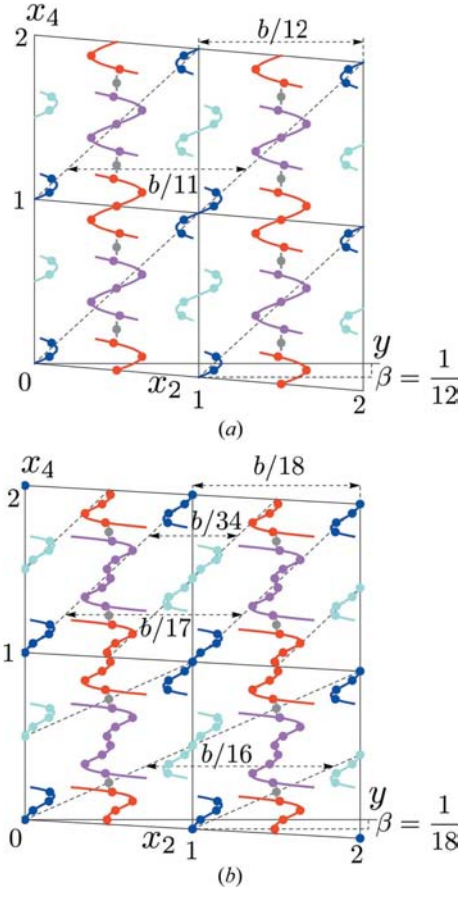

Figure 11
Projection (x_2, x_4) of the refined atomic domains with $x_3 = 0$ for the modular composite model of (*a*) lillianite and (*b*) heyrovskyite. The refined parameters are given in Table 9 of the supplementary material. Colour labels are as given in Figs. 8 and 9. The lines (dashed lines) corresponding to the competing periodicities discussed in the text are indicated.

For simplicity, and as the positional atomic modulations do not vary significantly when modulations of ADP's are introduced, Table 9 of the supplementary material and Table 6 list the results for the model with non-modulated ADPs for S1 and Pb1. The *R* values and the goodness-of-fit values obtained in the four- and three-dimensional refinements are very similar. However, there is a significant reduction in the number of parameters (reduction of 31 and 46% for lillianite and heyrovskyite, respectively). Except for the parameterization of the S1 atomic domain in the heyrovskyite compound, the reduction on the number of parameters originates from the use of common ADPs for all atoms associated with the same atomic domain.

The refined atomic domains are sketched in Figs. 11 and 12. The superspace model is represented in these figures using the setting corresponding to subsystem 0. One can see that the real structures deviate significantly from the idealized modules in a way that can be parameterized with a few harmonics. Note, however, that, due to the commensurability of the system, the only relevant values of the refined modulations are those corresponding to the discrete points indicated in the figures, which represent the actual atomic displacements realised in the real three-dimensional structure. The values of the modulation functions outside these points are irrelevant for the description of the structure, and depend in general on the parameterization employed for the modulation functions. In the present case, the use of the lowest harmonics introduces very long but irrelevant *tails* of the displacive modulations at the borders of the atomic domains. One can see in Table 9 of the supplementary material that there is no clear hierarchy among the harmonic functions used to describe the displacive modulation of each atomic domain. These two features are related, and can be avoided by an appropriate choice of the harmonics used for the description of the modulation (see §7).

Although the amplitudes of the refined individual harmonics are very large for some components, the actual global modulations with respect to the starting, perfect, modular structures are quite small with maximal displacements of the

order of 0.1–0.3 Å being somehow larger in the y direction than in the others. In Fig. 11 one must take into account that the basic unit cell used for the superspace construction is only ~ 1.7 Å along the y direction. Hence, the scale of these figures emphasizes the atomic displacements along y with respect to those along x, as depicted in Fig. 12. In the (x_1, x_4) plane the zigzag form of the atomic domains is essentially maintained, while in the (x_2, x_4) plane one can distinguish a clear tendency of the domains to orientate along the direction [0, 1, 0, 1] of the 3+1-dimensional space, as shown in the figures. This orientation was already present in the starting model of lillianite, but not in heyrovsyite (see Figs. 8*a* and 9*a*). As indicated in Fig. 11, in the case of heyrovskyite, perfect linear domains along the direction [0, 1, 0, 1] of the 3+1-dimensional space would correspond to an ordered arrangement of the atoms along the y direction separated by intervals of $b/17$, instead of the $b/18$ value introduced in the (3,5) ideal lattice used for the superspace construction. As there are 34 atoms in the $z = 0$ plane, this means that the system tends to produce an overall periodic sequence along y, with atomic positions separated by $b/34$, without making the distinction of the type of atom, Pb or S. These atoms, in fact, exchange their role in the approximate $b/34$ periodic sequence along y when passing from one module to the next. It thus seems clear that the choice of superspace embedding with $\beta = 1/(2N + 3)$ ($M = 2N + 3$) for the description of the composite would yield, in general, smaller modulations when seen in the global superspace setting. However, in this composite description the modulations of each subsystem are referred to its own average structure, and therefore their actual magnitude and parameterization will not change in practice. A simple way to take into account *a priori* this general tendency would be to introduce in the starting composite model a fixed linear sawtooth function with a slope corresponding to the [0, 1, 0, 1] direction of the 3+1-dimensional space for both the Pb and the S atomic domains. This would be convenient for heyrovskyite, but not necessarily in the case of lillianite, since here $3p + n = 2N + 3$, and the atomic domains already have the shape of sawtooth functions in the global superspace setting (see Fig. 8*a*).

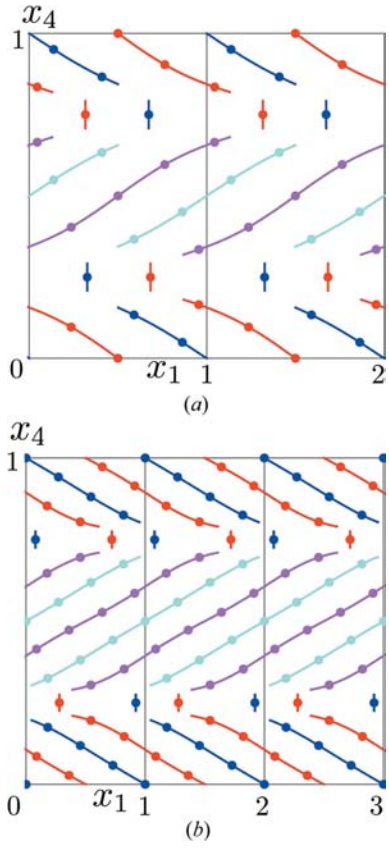

Figure 12
Projection (x_1, x_4) of the refined atomic domains with $x_3 = 0$ for the modular composite model of (*a*) lillianite and (*b*) heyrovskyite. The refined parameters are given in Table 9 of the supplementary material. Colour labels as in Figs. 8 and 9.

Another competing distance along y is $b/16$. This corresponds to a y equidistant configuration of the 16 Pb atoms. This periodicity leads to a slope given by the direction [0, 2, 0, 1] in the plane (x_2, x_4). It can be seen in Fig. 11(*b*) that this periodicity is also somehow latent in the configuration taken by the Pb atoms, especially considering the presence of the single Pb0 atom at $(x_2, x_4) = (1/2, 1/4)$. One can in fact make an alternative description considering the direction [0, 2, 0, 1] as the *existence line* in superspace for the Pb atoms, while keeping the vertical direction [0, 0, 0, 1] for the S atoms. This allows the introduction of continuous atomic domains for S and Pb. This way, we arrive at what we can call a *misfit* structure, where the misfit occurs between the set of ($b/18$ separated) S atoms and the ($b/16$ separated) Pb atoms. The modular character of the structure must then be introduced as an additional feature by aprioristic large zigzag modulations for the x_1 coordinate. This approach will be discussed in detail in §8.

7. The use of zigzag functions

It can be seen in Figs. 8 and 9 that the composite description developed above can in fact be considered equivalent to a single modulated structure with approximate sawtooth-like atomic domains, all of which are defined in the setting of subsystem 0. The approximate slopes of these atomic domains on the plane (x_1, x_4) correspond to well defined directions determined by the W matrices, namely directions $[3, \pm 1]$ and $[5, \pm 1]$ for lillianite and heyrovskyite, respectively. We can then describe the structure as a single modulated structure with a basic unit cell given by $\{a, b/(2N + 4), c\}$ and with a modulation wavevector $\mathbf{q} = \mathbf{b}^*$. The superspace group to be considered is $Bmmm(0, \beta, 0)s00$, the same as that used for the composite description and given in Table 3. A peculiar feature of the resulting superspace model is that the amplitudes of the necessary sawtooth modulations are very large, crossing several cells. These large amplitudes are however no obstacle in *JANA*2006 (Petříček *et al.*, 2006) for using a single modulated structure model. In this description we do not need to divide the structure into subsystems, so we do not require the introduction of the matrices W_1 and W_2 given above. Instead, the (fixed) amplitude of the sawtooth functions corresponding

to the ideal reference sublattice, shown in Figs. 8 and 9, should be introduced explicitly in the starting model and these amplitudes are dependent on the N value of the series member.

The description of the structure as a single modulated system has an important advantage. In Figs. 8(b) and 9(b), one can see that at least for the $x = x_1$ coordinate, the separation into different domains of the S0 and Pb0 atoms is quite artificial. Their positions are approximately continuous with those of the other two subsystems. They can be considered approximate vertices of a continuous zigzag function. In order to deal with this type of modulation, the use of continuous zigzag modulation functions has been implemented in *JANA*2006. These functions can now be parameterized in *JANA*2006 as shown in Fig. 13. One of the linear elements of the function is defined as it is usually done with sawtooth functions, namely by means of its centre along the internal space x_4^0, its width Δ and an amplitude $u_{0,i}^{zz}$ for each component. The second linear element of the function is then given by a sawtooth with opposite slope and centred at $x_4^0 + 1/2$. For $\Delta < 1/2$, the resulting function is almost equivalent to two symmetry-related sawtooth atomic domains, while for $\Delta = 1/2$ it produces a triangular function, as shown in Fig. 13(b). In fact, to our knowledge, the combination of two sawtooth functions to create a triangular atomic domain was used for the first time in the structure refinement of the incommensurately modulated phase of perylene (Lam *et al.*, 1995). However, the use of two symmetry-related and matched sawtooth functions produces double-valued points at the vertices and when the t section contains one of these vertices, the section gives rise to two atoms at the same position in the three-dimensional structure. This singularity is not a serious problem for incommensurately modulated structures, or even for a commensurate structure if the t section does not contain any of the vertices of the matched sawtooth but, for lillianite and heyrovskite, the relevant t section does contain the vertices of the zigzag, and it was necessary to modify *JANA*2006 to avoid double-valued points. The newly implemented zigzag option avoids these singularities and, therefore, the only difference between the zigzag functions and a couple of matched symmetry-related sawtooth functions are, precisely, the vertices.

As the different S atomic domains on the plane $x_3 = 0$ and within a unit cell occupy the whole x_4 interval without overlapping, one can describe all S atoms with a single atomic domain defined all along the internal space as a zigzag function with $\Delta = 1/2$ and only non-zero amplitude $u_{0,i}^{zz}$ along x. The value of $u_{0,1}^{zz}$ can be derived with the help of Figs. 1 and 2, considering the line of S atoms along the octahedra (coloured red in Fig. 1 and yellow in Fig. 2) between the layers at $y = 1/4$ and $y = 3/4$. There are $N + 2$ intervals separating S atoms, and the difference in the value of the x coordinate of consecutive atoms is close to 1/4. Therefore, the width along x_1 of each of the linear elements of the zigzag function is $(N + 2)/4$ and $u_{0,1}^{zz} = -(N + 2)/8$. The minus sign means that it has been chosen as x_4^0, the x_4 coordinate of the centre of the linear element with the negative slope (see Fig. 13).

The use of a zigzag function for S atoms not only reduces the number of independent S atomic domains in superspace to a single one, but also introduces a more efficient parameterization of the additional displacive modulation functions to be refined. The harmonics to be added are constrained by all operations of the superspace group and this avoids the spurious tails obtained in the composite model where the symmetry constraints for the modulation harmonics within each disconnected atomic domain are less restrictive.

In the case of the Pb atoms, the domains are not connected along x_4, and therefore one cannot define a single continuous atomic domain, but the two disconnected atomic domains Pb1 and Pb2 describing the Pb atoms within the two modules (treated as two different subsystems in the composite approach) can be described as a single zigzag function with $\Delta = N/(2N + 4) < 1/2$ (plus additional displacive harmonics to be refined). As in the case of the S atoms, the treatment of the two atomic domains as part of a single zigzag function introduces global symmetry constraints on the refinable displacive harmonics. A drawback of this model is that, as in the composite description, the Pb0 atom has to be treated separately as a single *monoatomic* domain.

The results of the refinements of the lillianite and heyrovskyite structures within this approach, *i.e.* as single modulated structures with zigzag functions, are equivalent to those

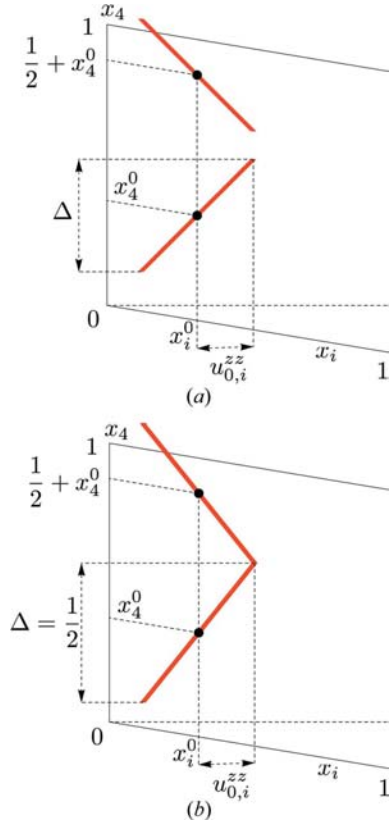

Figure 13
Parameters in the new option of *JANA*2006 describing a zigzag function: (a) case $\Delta < 0.5$; (b) case $\Delta = 0.5$ corresponding to a continuous zigzag line.

Table 7
Atomic domains in superspace defining an ideal $^{N,N}L$ member of the lilllianite homologous series within the Pb–S misfit composite model (choice $M = 2N + 3$ and superspace group of the second column of Table 3).

The positions of the centres of the atomic domains plus their widths Δ along x_4, and values of the zigzag function along x_1 ($u^{zz}_{0,1}$) are listed. In the last two columns, the point symmetry of the centre of the atomic domain and the corresponding form of the displacive modulation (odd sine terms and even cosine terms for the x and y components of the modulation, and no modulation at all for the z component) are included. The matrices of the first, second and third subsystems are the identity, W_+ and W_-, respectively.

Atom	Subsystem	x^0_1	x^0_2	x^0_3	x^0_4	Δ	$u^{zz}_{0,1}$	Point symmetry	Displacive modulation
S	1	1/2	1/2	0	0	1/2	$-(N+2)/8$	*mmm*	(sin(odd),sin(even),0)
Pb	2	0	0	0	0	1/2	$-(N+1)/8$	*mmm*	(sin(odd),sin(even),0)

$$W_{\pm} = \begin{pmatrix} 1 & 0 & 0 & 0 \\ 0 & 1 & 0 & \pm 1 \\ 0 & 0 & 1 & 0 \\ 0 & 0 & 0 & 1 \end{pmatrix}$$

reported above for the composite approach. In contrast to the composite approach, ADPs of S0 are quite different from those of the other S atoms. Consequently, in this case a modulation of these ADPs for the S domain is important to reach an optimal fit. Note that in the refinements the parameters of the two zigzag functions were fixed, as they are the reference which corresponds to the idealized modules discussed in previous sections and only displacive harmonics were refined. In any case, a refinement of the parameters describing the zigzag function is not advisable since they would be strongly correlated with the first harmonic of the refined displacive modulation function. Tables with the details of these refinements can be found in the supplementary material (Tables 10 and 11). A graphical scheme of the final refined model of heyrovskyite can be seen in Fig. 14. Although the points in superspace defining the actual atomic positions in real space are essentially identical to those of the composite refinement, the modulations of the continuous functions defining the associated atomic domains are smoother and better behaved. This should make these functions more invariant to composition, *i.e.* more transferable to other more complex compositions.

8. Lillianite and heyrovskyite within a Pb–S misfit composite model

The results obtained so far suggest a third approach to the superspace description of these structures. It should be possible to treat them as a conspicuous misfit compound, with one subsystem formed by the S atoms and a second one by the Pb atoms. We have seen above that the y coordinates of the S and Pb atoms within a (x, y) layer, when seen in superspace, tend to form an approximate equidistant array with the period $b/(2N + 3)$ within the modules. This feature is again highlighted in Fig. 14 for the case of heyrovskyite. The number of S and Pb atoms within the supercell is, however, $2N + 4$ and $2N + 2$, respectively, and, as pointed out earlier, this composition misfit is at the origin of the compound series. While chemically a 1:1 proportion of S and Pb atoms is preferred on a local basis, the system is forced to accommodate the Pb deficit corresponding to the actual composition stemming from the introduction of a cation with a higher valence (Bi for Pb).

It is therefore desirable to devise a starting reference structure in superspace which stresses this misfit between S and Pb atoms. For this model the description of the S atoms is maintained, *i.e.* a basic unit cell $\{a, b/(2N + 4), c\}$, a wavevector $\mathbf{q} = \mathbf{b}^*$ and a single independent zigzag function. The Pb atoms, however, are now considered as forming a second subsystem with the basic unit cell $\{a, b/(2N + 2), c\}$ and a modulation wavevector of $\mathbf{q} = \mathbf{b}^*$, so that in the starting non-modulated basic structure the y coordinates of the $(2N + 2)$ Pb atoms are equidistant. This description represents the introduction of a new concept for the treatment of these compounds as composites, as now the subsystems are not formed by the modules, but by the Pb and S atoms, respectively. In Fig. 14 this composite misfit Pb–S approach corresponds to considering a continuous existence line for the Pb atoms along the superspace direction [0, 2, 0, 1], if the structure is described in the setting of the S subsystem.

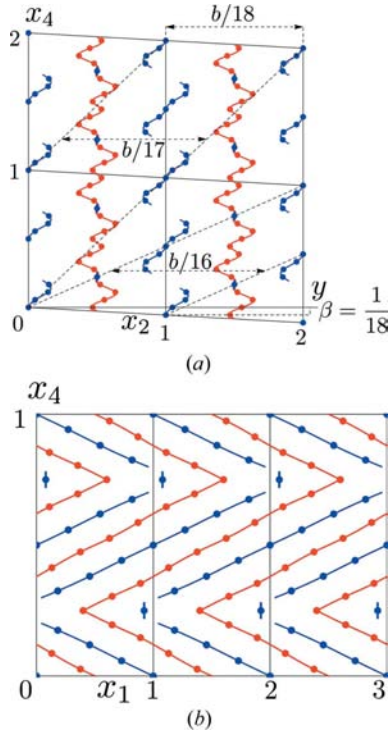

Figure 14
Projections (*a*) (x_2, x_4) and (*b*) (x_1, x_4) of the refined atomic domains with $x_3 = 0$ for the model of §7. The structural and refined parameters are given in Tables 10 and 11 of the supplementary material, respectively.

The three-dimensional positions of the $(2N + 2)$ Pb atoms can now be described with a single independent atomic domain, which includes the Pb0 atoms and this, in turn, allows the introduction of a continuous triangular zigzag modulation function for the Pb atomic domain within its particular basic unit cell as the starting model for refinement. The amplitude of this zigzag function is given by $u^{zz}_{0,1} = -(N + 1)/8$, which can be readily derived using the same arguments of the preceding section for the amplitude of the S atomic domain.

Fig. 15 shows the resulting starting model for refinement in superspace and Fig. 16 depicts the corresponding structure in real space for heyrovskyite. In this structure the modules, while keeping locally the right topology, deviate considerably from the archetype substructure. The approximate galena modules should then be recovered by the additional displacive atomic modulations to be refined. In other words, while in the composite description of §6 the modulations essentially describe deviations of the modules from the defined idealized sublattices close to the galena structure, the modulations here should in fact approximate the more distorted modules to the ideal galena structure, starting from a reference structure, where a regular separate distribution of S and Pb atoms is considered. Note that this composite model has a peculiar feature: in contrast with the usual incommensurate composites, an *a priori* fixed modulation function along x is included in the starting model for both subsystems, as given by the two zigzag functions.

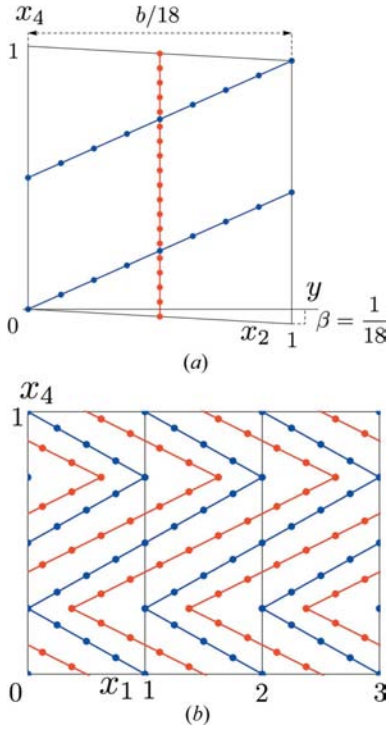

Figure 15
(*a*) (x_2, x_4) and (*b*) (x_1, x_4) projections of the starting refinable model in the misfit composite approach given in Table 7 for heyrovskyite. The setting used for the superspace is that of the S subsystem. Colour labels as in Figs. 8 and 9.

From the results obtained earlier we know that the S and Pb atoms tend to form arrangements with y coordinates equidistant by $b/(2N + 3)$ within the modules. It is therefore convenient to use this distance, $b_{\rm av} \equiv b/(2N + 3)$, intermediate between those favoured by S and Pb atoms, as the reference basic lattice for the superspace construction. We therefore introduce in *JANA*2006 a subsystem 0 with no atoms but with its basic lattice given by $\{a, b_{\rm av} \equiv b/(2N + 3), c\}$ and a modulation wavevector $\mathbf{q} = \mathbf{b}^*$. This first subsystem determines the basis of four reciprocal vectors to be used for the definition of the other subsystems by means of their W matrices. The reciprocal bases considered for the S and Pb subsystems differ only in the choice of the reciprocal basic lattice vector along y. For the S subsystem $b^*_{\rm S} = (2N + 4)b^* = b^*_{\rm av} + b^*$, while for the Pb subsystem $b^*_{\rm Pb} = (2N + 2)b^* = b^*_{\rm av} - b^*$. Therefore, the corresponding W matrices are very simple. They are given in Table 7, together with the parameters that define the single independent atomic domains associated with each subsystem. In the setting of subsystem 0 the superspace group to be considered is $Bbmm(0, \beta, 0)s00$, listed in the second column of Table 3. Fig. 17 shows the same starting model as shown in Fig. 15 for heyrovskyite but using this intermediate basic unit cell. Only the (x_2, x_4) projection is shown, since the other projection on the plane (x_1, x_4) does not change. The existence line of the S atoms now follows the oblique direction $[1, -1]$ within the (x_2, x_4) plane, which corresponding to a longer diagonal within the unit cell and gives rise to 18 (*i.e.* $2N + 4$) atomic positions, while the Pb existence line follows the $[1, 1]$ direction, resulting in only 16 distinct atomic positions per atomic domain. The use of this intermediate superspace setting by means of a void zeroth subsystem does not mean any change in the parameterization of the modulations in subsystems S and Pb, as the modulations in these subsystems are defined with respect to their own superspace bases.

There are important differences between the misfit composite model and the other two approaches used in the present work. The difference between the modular composite and misfit composite approach are the subsystems considered. While in the composite modular model the two subsystems are two Pb–S galena blocks with different orientations, in the misfit composite approach S and Pb atoms are separated into two different subsystems. The intermediate model of §7 is a purely modulated model (no composite approach) with zigzag functions for both S and Pb. The difference with the the S–Pb misfit composite model used in this section is not only that in one case the zigzag function of Pb is broken and the other not, but that in the misfit composite model the system is treated as a composite and the Pb is taken as a second subsystem with its own average periodicity along the y axis different from that of S (this is what allows us to make a continuous zigzag function for Pb). However, in the intermediate model the average periodicity along the y axis is the same for S and Pb, and this necessarily forces the atomic domains of Pb along the internal space to be discontinuous, with some voids.

Refinements of lillianite and heyrovskyite within the misfit composite model converged smoothly. The results are

summarized in Table 6 and Table 12 of the supplementary material, and are depicted in Figs. 18 and 19, where they are represented using the setting of subsystem 0. The atomic positions corresponding to the inner part of the modules have been highlighted in the figure. In the case of heyrovskyite one can clearly see how these atoms arrange regularly along the y axis with an intermediate distance of $b/17$. Especially the Pb atoms deviate very little from a vertical configuration along x_4 (one should note that the basic unit cell along y is of the order of 1.8 Å). In the case of the S atoms, the influence of the interface between modules affects not only the atom positioned at the interface, but also the two neighbouring ones. In the case of the modulation functions along x_1, the refinement has introduced the expected parallelism between the zigzag functions of S and Pb atoms, which the starting misfit model lacked (see Fig. 15*b*). This, together with the approximate $b/17$ periodicity along the y direction, produces the approximate regular galena structure of the modules present in the real structure (Fig. 2).

Although under this approach the modulations added to the starting model are rather large, the refinements behaved well. It can be seen in Table 12 of the supplementary material that, in contrast with the refinement carried out under the modular composite model, the amplitudes of the refined harmonics keep a clear hierarchy depending on their order. While in lillianite the atomic domains in superspace describe too small a number of atomic positions in real space, in the case of heyrovskyite this number is sufficiently large for the superspace description to be more efficient and economical than the conventional approach. The number of parameters refined to describe the positional modulations is 12, while a conventional approach requires 16. The four and five crystallographically independent positions of the Pb and S atoms can be described by six harmonic amplitudes in each case. However, the number of ADPs for the Pb atom is larger than the total number of ADPs of the Pb0 and Pb1 atoms in the modular composite approach. The atoms which belong to the Pb1 atomic domain in the composite approach are inside the shaded regions of the Fig. 18, *i.e.* inside the galena blocks. They have similar neighbourhoods and, consequently, the use of a common ADP is sufficient (Table 9 of the supplementary material). However, the Pb0 atom has a very different neighbourhood and, as a consequence, different ADPs. In the misfit composite model, in which all the Pb atoms belong to the same atomic domain, modulations of the ADPs are necessary to reproduce the variation of these parameters for different atoms in the resulting three-dimensional structure. This can be a serious problem for higher members of the

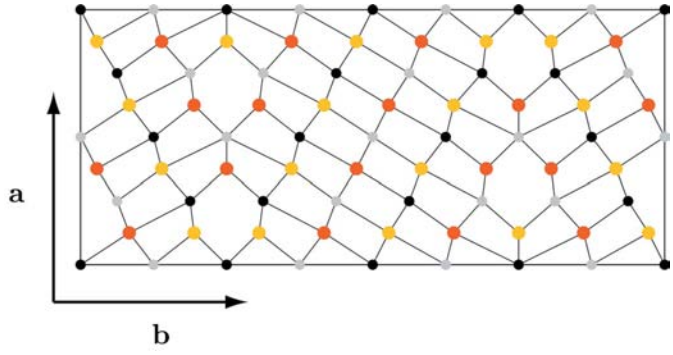

Figure 16
Idealized heyrovskyite for the misfit composite model (without displacive modulations). The meaning of the colour and atom sizes are the same as in Figs. 1 and 2.

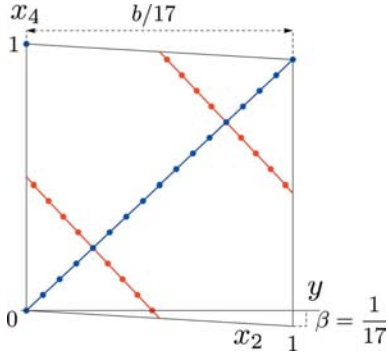

Figure 17
(x_2, x_4) projection of the starting model in the misfit composite approach given in Table 7 (equivalent to Fig. 15), but in the setting intermediate between those of the S and Pb subsystems. In this setting, the (x_1, x_4) projection is identical to that given in Fig. 15.

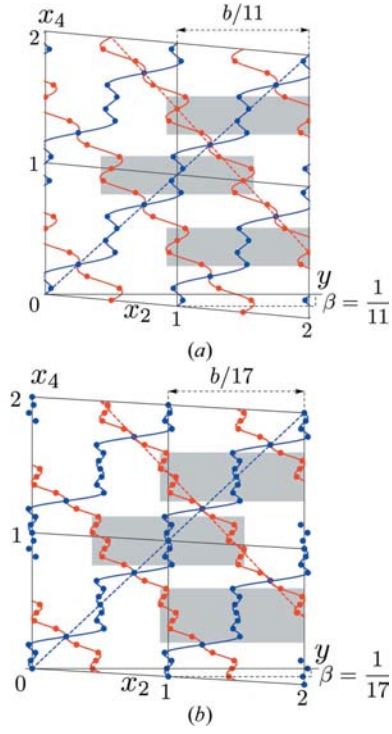

Figure 18
Projection (x_2, x_4) of the refined atomic domains with $x_3 = 0$ for the misfit composite model of (*a*) lillianite and (*b*) heyrovskyite. The refined parameters are given in Table 12 of the supplementary material. Colour labels as in Figs. 8 and 9. The lines corresponding to a periodicity (*a*) **b**/10 (blue) and **b**/12 (red) and (*b*) **b**/16 (blue) and **b**/18 (red) are indicated. Shaded regions represent the slightly distorted galena blocks inside the modules (see Figs. 1 and 2).

series. In some cases it could be convenient to separate the Pb atomic domain in two parts to avoid the inclusion of a large number of Fourier terms to force the modulation to be a step-like function.

The *R* factors obtained are comparable to those obtained in the modular composite approach and in the three-dimensional refinements (see Table 6). What is even more important is that judging from the aspect of the modulation functions of heyrovskyite as shown in Figs. 18 and 19, one expects that these modulations will be fairly invariant when compounds with larger modules are considered. This opens the possibility of refining more complex members of the series having larger unit cells such as ourayite ($^{[11,11]}L$), without a significant increase of the refinement parameters.

9. Conclusions

We have shown that the lillianite compounds, a homologous series of modular structures with two identical symmetry-related modules of variable size and having two different orientations, can be efficiently described and refined as commensurate modulated structures using the tools of the superspace formalism, originally developed for incommensurate modulated structures. Three alternative superspace models have been successfully applied. First, a so-called modular composite model has been used, in which the structure is described as a modulated composite with two basic subsystems formed by the atoms belonging to each type of module. However, in this model the atoms at the interface between modules had to be treated separately. A second model as a single modulated structure is also possible if so-called linear zigzag functions with large amplitudes are introduced in the parameterization of the atomic modulations. Finally, the use of these zigzag functions allows us to introduce a third description of the structures as misfit composite materials where the cations form one subsystem and the anions form the other one. This third approach appears to be the most robust and efficient, as the sets of all cations and anions are described by single independent atomic domains. While all three models allow refinements comparable with those of conventional three-dimensional methods, especially the last model requires fewer refinable parameters and, in addition, their number does not scale with the size of the unit cell. The methodology can in principle be extended to other compound families with similar modular features, and opens new possibilities for the structural analysis of compounds in series with very large unit cells.

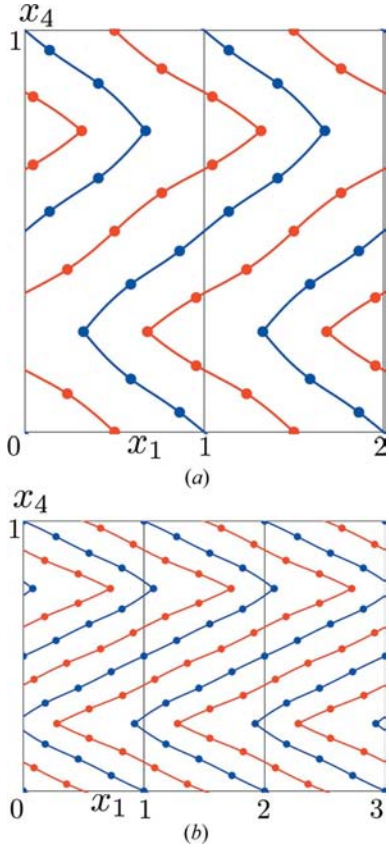

Figure 19
Projection (x_1, x_4) of the refined atomic domains with $x_3 = 0$ for the misfit composite model of (*a*) lillianite and (*b*) heyrovskyite. The refined parameters are given in Table 12 of the supplementary material. Colour labels as in Figs. 8 and 9.

APPENDIX *A*
Optimal sublattices for a modulated description

In §4 it was shown that the reference galena sublattice to be used in a modulated composite description of the structures is defined by a pair of integers (n, p) and equations (2). The

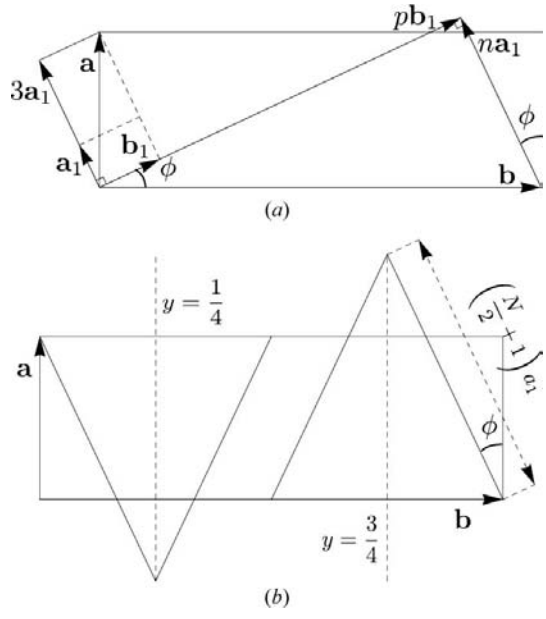

Figure 20
(*a*) Scheme of the geometrical relation connecting the unit cell of the global structure and the magnitudes of the sublattice vectors defined by (2), for an ideal unstrained sublattice, and a global orthogonal unit cell. (*b*) Relation between (n, p) and N, and determination of the b parameter of the global unit cell in the case of ideal unstrained sublattices of the $^{N,N}L$ member of the series.

optimal (n, p) values that would yield the least strained sublattice with respect to that of the ideal gallena can be calculated as follows.

In an ideal sublattice, unstrained with respect to the galena lattice, the ratios $a_{1,2}/c_{1,2}$ and $b_{1,2}/c_{1,2}$ are 1 and $2^{1/2}$, respectively, and the lattice is orthogonal. Fig. 20(a) shows a scheme of the geometrical relation connecting the unit cell of the global structure and the magnitudes of the sublattice vectors defined by (2), in the specific case of an ideal unstrained sublattice, and a global orthogonal unit cell. One can see that necessarily $b_1/3a_1 = na_1/pb_1$ and, therefore, considering that $b_1 = 2^{1/2}a_1$, for this particular unstrained situation, the (n, p) values should satisfy (4).

On the other hand, in a fully unstrained situation for the sublattices corresponding to an ${}^{N,N}L$ member of the series, the indices (n, p) can be related with N, as shown schematically in Fig. 20(b). The parameter b of the global unit cell would be given by

$$b = (2N + 4)a_1 \sin\varphi. \tag{12}$$

Alternatively, from Fig. 20(a), one can write

$$b = 2^{1/2}pa_1 \cos\varphi + na_1 \sin\varphi. \tag{13}$$

Considering that $\tan\varphi = 2^{1/2}/3$, the compatibility of the two equations implies equation (5).

In general, (4) and (5) cannot be satisfied at the same time with integer (n, p) values. The best option can be obtained considering the integer values which are closer to the non-integer solution of these equations.

This work has been supported by the European Mineral Initiative of the European Science Foundation (project EuroMinsci-ORION), MEC-Spain, UPV/EHU, the Czech Science Foundation (No. 202/06/0757) and the Danish Natural Science Research Council. Some of the authors (LE, JMPM and KF) also gratefully acknowledge the support obtained as research group from the Basque Government (ref: IT-282-07). We would like to thank E. Makovicky for his detailed comments on a first version of the article, and for having pointed out to us that the sublattices considered in a modular description are not in general coherent.

References

Bruker AXS Inc. (2000). *Software Reference Manual*. Bruker AXS Inc., Madison, Wisconsin, USA.
Boullay, P., Trolliard, G., Mercurio, D., Perez-Mato, J. M. & Elcoro, L. (2002). *J. Solid State Chem.* **164**, 261–271.
Darriet, J., Elcoro, L., Abed, A. E. & Perez-Mato, J. M. (2002). *Chem. Mater.* **14**, 3349–3363.
Elcoro, L. & Perez-Mato, J. M. (1996). *Phys. Rev. B*, **54**, 12115–12124.
Elcoro, L., Perez-Mato, J. M. & Withers, R. (2000). *Z. Kristallogr.* **215**, 727–739.
Elcoro, L., Perez-Mato, J. M. & Withers, R. L. (2001). *Acta Cryst.* B**57**, 471–484.
Evain, M., Boucher, F., Gourdon, O., Petříček, V., Dusek, M. & Bezdicka, P. (1998). *Chem. Mater.* **10**, 3068–3076.
Ferraris, G., Makovicky, E. & Merlino, S. (2004). *Crystallography of Modular Materials.* Oxford University Press.
Gostojić, M., Nowacki, W. & Engel, P. (1982). *Z. Kristallogr.* **159**, 217–224.
Janner, A. & Janssen, T. (1980*a*). *Acta Cryst.* A**36**, 399–408.
Janner, A. & Janssen, T. (1980*b*). *Acta Cryst.* A**36**, 408–415.
Janssen, T., Chapuis, G. & de Boissieu, M. (2007). *From Modulated Phases to Quasicrystals.* Oxford University Press.
Janssen, T., Janner, A., Looijenga-Vos, A. & de Wolf, P. M. (1992). *International Tables for Crystallography*, edited by A. J. C. Wilson, Vol. C, pp. 797–835. Dordrecht: Kluwer Academic Publishers.
Lam, E. J. W., Beurskens, P. T., Smits, J. M. M., van Smaalen, S., de Boer, J. L. & Fan, H.-F. (1995). *Acta Cryst.* B**51**, 779–789.
Landa-Canovas, A. & Otero-Diaz, L. (1992). *Aust. J. Chem.* **45**, 1473–1487.
Lemoine, P., Carré, D. & Guittard, M. (1986). *Acta Cryst.* C**42**, 390–391.
Lind, H. & Lidin, S. (2003). *Solid State Sci.* **5**, 47–57.
Makovicky, E. & Balić-Žunić, T. (1993). *Neues Jahrb. Miner. Abh.* **165**, 317–330.
Makovicky, E. & Karup-Møller, S. (1977*a*). *Neues Jahrb. Miner. Abh.* **130**, 264–287.
Makovicky, E. & Karup-Møller, S. (1977*b*). *Neues Jahrb. Miner. Abh.* **131**, 56–82.
Makovicky, E. & Karup-Møller, S. (1984). *The Canadian Mineralogist* **22**, 565–575.
Michiue, Y., Yamamoto, A., Onoda, M., Sato, A., Akashi, T., Yamane, H. & Goto, T. (2005). *Acta Cryst.* B**61**, 145–153.
Michiue, Y., Yamamoto, A. & Tanaka, M. (2006). *Acta Cryst.* B**62**, 737–744.
Orlov, I., Palatinus, L., Arakcheeva, A. & Chapuis, G. (2007). *Acta Cryst.* B**63**, 703–712.
Perez-Mato, J., Elcoro, L., Aroyo, M. I., Katzke, H., Tolédano, P. & Izaola, Z. (2006). *Phys. Rev. Lett.* **97**, 115501.
Perez-Mato, J., Elcoro, L., Petříček, V., Katzke, H. & Blaha, P. (2007). *Phys. Rev. Lett.* **99**, 025502.
Perez-Mato, J. M., Zakhour-Nakhl, M., Weill, F. & Darriet, J. (1999). *J. Mater. Chem.* **9**, 2795–2808.
Petříček, V., Dusek, M. & Palatinus, L. (2006). *JANA*2006. Institute of Physics, Prague, Czech Republic.
Petříček, V. & Makovicky, E. (2006). *Can. Mineral.* **44**, 189–206.
Pinto, D., Balić-Žunić, T., Garavelli, A., Makovicky, E. & Vurro, F. (2006). *Can. Mineral.* **44**, 159–175.
Smaalen, S. van (1991). *Phys. Rev. B*, **43**, 11330–11341.
Smaalen, S. van (2007). *Incommensurate Crystallography.* Oxford University Press.
Takagi, J. & Takéuchi, Y. (1972). *Acta Cryst.* B**28**, 649–651.
Takeuchi, Y. & Takagi, J. (1974). *Proc. Jpn Acad.* **50**, 76–79.
Wolff, P. M. de (1974). *Acta Cryst.* A**30**, 777–785.